

^1H NMR Relaxometry in the TGBA* and TGBC* Phases.

Valentina Domenici,^{*1} Anton Gradišek,² Tomaž Apih,³ Vera Hamplova,⁴ Vladimira Novotna⁴ and
Pedro J. Sebastião^{5,6}

1. Dipartimento di Chimica e Chimica Industriale, Università degli studi di Pisa, via Moruzzi 13,
56124 Pisa, Italy

2. EN-FIST Centre of Excellence, Dunajska 156, SI-1000 Ljubljana, Slovenia

3. Jozef Stefan Institute, Jamova 39, SI-1000 Ljubljana, Slovenia

4. Institute of Physics, Academy of Sciences of the Czech Republic, Na Slovance 2, 182 21 Prague,
Czech Republic

5. Departamento de Física, Instituto Superior Técnico, Universidade de Lisboa
Av. Rovisco Pais, 1049-001 Lisboa, Portugal

6. Center of Physics and Engineering of Advanced Materials, Instituto Superior Técnico
Universidade de Lisboa, Av. Rovisco Pais, 1049-001 Lisboa, Portugal

(Received:)

*Corresponding author (E-mail: valentina.domenici@unipi.it)

Abstract

In this work, recent results obtained by means of ^1H NMR relaxation studies of liquid crystals having a large range of thermal stability of the twist grain boundary (TGB) phases are reviewed. In particular, three chiral rod-like lactate derivative mesogens, with the same chiral lateral chain, were investigated from the molecular dynamics point of view. In the isotropic phase, a three-exponentials magnetization decay was observed and the three relaxation times were assigned to three specific nuclear spin groups of these molecules (i.e. aromatic core, methyl and methylene groups). In the liquid crystalline phases the magnetization decay detected was mono-exponential and a single spin-lattice relaxation times (T_1) was measured at each temperature. Focusing in the TGBA* and TGBC* phases, the main features of the dispersion curves (spin-lattice relaxation rates as a function of the Larmor frequency) in terms of molecular dynamics are here discussed and compared.

Keywords: ferroelectric liquid crystal, chiral liquid crystals, molecular dynamics, nuclear magnetic resonance (NMR), twist grain boundary phases, spin-lattice relaxation.

Running head: TGB Phases by ^1H NMR relaxometry.

1. Introduction

Twist grain boundary (TGB) liquid crystals [1] represent a fascinating example of interplay between molecular chirality, volume-excluded and energetic balances related to the occurrence of helical supramolecular arrangements. In these phases, chiral molecules pack in layers, as in typical SmA or SmC* phases, but, at a domain level, these layers form helical structures in a discontinuous way, giving rise to grain boundaries (see **Scheme 1**). [3,4] Since the first investigations based on X-ray and microscopy, coupled with theoretical models [1-4], the structural details of both TGBA (having a SmA-like domain structure) and TGBC* (with local SmC or SmC* layer structures) have been recently confirmed by ^2H NMR studies [5,6]. These works [5,6] put in evidence the delicate nature of TGB phases and their supramolecular structure, which can be deformed or unwound by external magnetic and electric fields, ~~such as magnetic and electric ones~~. Moreover, in most of the chiral liquid crystals having TGB phases, these mesophases are stable but often observed in short temperature ranges of few degrees, thus making their investigation hard. ~~being complicate to investigate.~~

However, in the recent years, our group had the chance to investigate several compounds showing TGBA and TGBC* phases stable in wide temperature ranges [7,8]. Besides the structural features of TGB phases, we investigated the main molecular dynamic processes ~~active~~ in these phases by means of ^1H NMR relaxometry [9,10].

This technique is extremely powerful in detecting and characterizing both slow and fast motions in liquid crystals [9-17]. By measuring the proton spin-lattice relaxation time (T_1) over a wide range of Larmor frequencies, from a few kHz to hundreds of MHz, it is possible to identify single molecular motions, overall and internal ones, translational self-diffusion and collective motions, which are very typical of liquid crystals. Among those, order director fluctuations (ODF), in nematic phases [14,15], and layer undulations (LU), in smectic phases, have been widely explored by these techniques in several liquid crystalline systems [12,17]. Additionally, rotations mediated by translational displacements (RMTD) have also been investigated by NMR relaxometry [12].

In this paper, we are reporting the main results obtained by ^1H NMR relaxometry applied to three rod-like mesogens having TGB phases stable in wide temperature ranges. The three

molecular systems have the same chiral lateral chain, based on the (S)-2-methylbutyl-(S)-lactate unit [7,8], but different achiral lateral chains and/or aromatic cores. Two of these systems have been analyzed in two independent works [9,10]. Here, the addition to the analysis of a third compound we take the opportunity to make some more general comments on both TGBA and TGBC* dynamics.

2. Experimental

The molecular structure of the three chiral liquid crystals is reported in **Scheme 2**. Two of them, HZL 7/* and HZL 9/* differ only for the number of carbons on the achiral lateral chain, while the 10BBL system has a completely different aromatic core. Their polymorphisms, determined by differential scanning calorimetry (DSC), on cooling from the isotropic phase, at a scan rate of 10°/min are here reported:

HZL 7/ mesogen:*

Iso - 123 °C - N* - 120 °C - TGBA* - 86 °C - TGBC₁* - 70 °C - TGBC₂* - 27 °C crystal

HZL 9/ mesogen:*

Iso - 120 °C - N* - 111 °C - TGBA* - 95 °C - TGBC₁* - 80 °C - TGBC₂* - 66 °C crystal

10BBL mesogen:

Iso - 122 °C - BP - 118 °C - TGBA* - 108 °C - TGBC* - 99 °C - SmC* - 53 °C crystal

The HZL 7/* and HZL 9/* samples present the same mesophases, but different temperature transitions. Both HZL samples have a cholesteric phase (N*) below the isotropic phase, while the 10BBL has a blue phase (BP). Moreover, the 10BBL mesogen shows only one type of SmC*-like TGB phase, named here TGBC* phase, while the two HZL mesogens have two types of SmC*-like TGB phase, named here TGBC₁* and TGBC₂* phases.

^1H -NMR experiments were performed on a Fast Field Cycling NMR relaxometer SPINMASTER FFC-2000 (Stelar s.l.r.). All details for the samples HZL 7/* and 10BBL are reported in refs. [9] and [10], respectively. For the HZL 9/* compound, about 500 mg of the sample was used for the measurement. AND FOR THE OTHER SAMPLES? The proton longitudinal spin-lattice relaxation times T_1 were measured in the frequency range from 18 MHz to 5 kHz. Above 5 MHz, the non-prepolarized (NPS) pulse sequence was used for relaxation measurements, while below that frequency a prepolarized (PPS) pulse sequence was used. The prepolarization and acquisition frequencies were 18 and 9.25 MHz, respectively. A 6.5 μs proton spin 90° pulse was used. All other parameters were optimized according to each experiment.

The temperature dependency of proton T_1 was measured at the Larmor frequency (I WOULD USE ν_L as ω_L is for angular frequency...) ω_L of 100 MHz over a wide temperature range using a home-built spectrometer and an Oxford superconducting magnet. The inversion recovery pulse sequence with a 2.2 μs proton spin 90° pulse was used.

3. Results and Discussion

3.1 Relaxation behaviour in the isotropic phase

As observed for HZL 7/* and 10BBL liquid crystals in previous works [9,10], also in the HZL 9/* compound, we could observe that in the isotropic phase there were three components in relaxation behavior. These relaxation components can be attributed to different proton spin groups, namely methyl, methylene and aromatic ones. In order to separate these components, different parts of the ^1H NMR spectra were integrated, corresponding to different groups. As it can be clearly seen in **Figure 1 (a)**, in the isotropic phase the ^1H NMR spectrum of HZL 9/* recorded at $\omega_L=100\text{MHz}$ is composed by different signals that can be separated: the aromatic signals, and the CH_2 and CH_3 proton signals. When the sample is cooled down to the mesophases, the ^1H NMR spectra are dominated by a broad signal (see **Figure 1(b)** and **1(c)**) and the different components cannot be separated anymore. On the other hand, the relaxation behavior is characterized by a mono-exponential trend, giving rise to a single relaxation time.

In **Figure 2** the temperature dependences of the measured relaxation times of the three compounds are reported. As previously said, the isotropic phase is characterized by three

components, while the relaxation rate in the TGB phases presents a monotonous increase by decreasing the temperature for all samples. In the case of HZL 7/* the relaxation trends in the cholesteric phases (N*) are also not mono-exponential, while in the HZL 9/* the relaxation behavior is mono-exponential in the N* and TGB* phases. Similarly, the 10BBL shows a single relaxation behavior in the blue phase (BP), TGB* and SmC* phases.

3.2 Relaxation mechanisms in the TGBA and TGBC* phases

Typical dispersion curves, namely relaxation rates $R_l (=1/T_l)$ as a function of the Larmor frequency (ω_L), recorded in the TGBA* and TGBC* phases of the two compounds HZL 7/* and HZL 9/* are reported in **Figure 3**. These curves are typical of TGB phases, as reported in ref. [9,10], and reflect the particular supramolecular structure of the twist grain boundary phases, as shown in **Scheme 1**.

The dispersion curves recorded in the TGBA* phases, and reported in **Figure 3(A)**, are quite similar between the two mesogens in the fast and intermediate regions, while, in the low frequency regime, the relaxation times are shorter in the HZL 9/* with respect to the HZL 7/*. As it is clear from the analysis of dispersion curves in terms of dynamic processes, this can be explain by the presence of slower motions in HZL 9/* with respect to HZL 7/*, which can be understandable since the HZL 9/* sample is longer than HZL 7/*.

In the case of TGBC* phases, the HZL 9/* sample is characterized by similar dispersion curves in both TGBC₁* (grey symbol in **Figure 3(B)**) and TGBC₂* (black symbol in **Figure 3(B)**), thus indicating that, in this case, there shouldn't be significant differences between the two phases. On the contrary, the HZL 7/* sample, which presents TGBC* phases at much lower temperatures than HZL 9/*, presents dispersion curves very different in the TGBC₁* and TGBC₂* phases. On the other hand, the dispersion curve of HZL 7/* in TGBC₂* phase, recorded at 40°C, reflects the presence of a slightly larger rigidity of the phase structure with respect to the TGBC₁* phase, as reported in ref. [10], and this is more clearly inferred from the quantitative analysis of relaxation times in terms of dynamic motions.

The total spin-lattice relaxation rate $R_l (=1/T_l)$ can be analyzed by assuming that each motional contribution can be considered statistically independent from the others, or otherwise its characteristic time of the molecular motions reasonably different from the others. In this respect, the

total measured R_I can be defined as a sum of different contributions, i , corresponding to the different relaxation mechanisms [12,13], according to Eq.[1]:

$$\frac{1}{T_1(\omega)} = \sum_i \frac{1}{T_{1,i}(\omega)} \quad [1]$$

Where the subscript i corresponds to:

1) R, to represent local molecular Rotations, such as fast spinning reorientations or internal motions (R_f) and slower ones, such as tumbling reorientations (R_t). These motions are usually modeled by means of the Bloembergen, Purcell, and Pound (BPP) relaxation theory [16]. For each type of rotational contribution, two parameters can be optimized: the correlation time, τ_R , and the pre-factor, A_R .

2) SD, to indicate the translational Self-Diffusion motion. In our approach, the SD contribution was described by the model described in ref.[18], and it is defined by a correlation time τ_D and an activation energy E_D .

3) CM, to indicate the collective motions, which are typical of the liquid crystalline phases and are characterized by different distributions of fluctuation modes with amplitudes and damping times related to the anisotropic viscoelastic properties of these compounds. These CMs are: the Order Director Fluctuations (ODFs) typical of nematic phases; the Layer Undulations (LU) present in the SmA and other smectic-like phases, and in-plane fluctuations around the tilt director, (cDF), (e.g. azimuthal fluctuations of the tilt direction in the smectic C layers), in SmC* phases [12,13].

4) RMTD, to indicate the Rotations Mediated by the Translational Displacements, that were introduced to explain the relaxation process associated with rotations that are induced by the diffusion of molecules along the helical axis, as in the case typical of chiral mesophases, such as the Cholesteric (N*) and TGB* phases, . With respect to the RMTD across the TGB grain-boundaries, the model was proposed by Vilfan *et al.*[17] and this contribution depends on the value of the helical pitch, p , and on the translational diffusion coefficient, D .

In order to analyze the experimental dispersion curves, we assume that the correlation times typical of each motional contribution are energetically activated, and, in particular, Arrhenius trends are assumed. Moreover, in order to avoid the number of fitting parameters becoming too large, in our approach, some parameters were estimated according to data available for the mesogens under

investigation, such as the orientational order, geometrical and conformational features and tilt angle, and kept fixed in the least square minimization fitting procedure.

The fitting of the dispersion curves in the TGBA* phase was performed for all mesogens by considering the above motional processes. In both HZL samples and in the 10BBL mesogen, the values of the fitting parameters are very similar to those referred to in the literature for the SmA phase, except that in the low frequency regime. In fact, at lower frequencies, the R_I trend is better fitted by a stronger contribution of the RMTD relaxation mechanism, as shown in **Figure 4(a)**. Moreover, in the fitting procedure, LUs were also included and they represent a minor contribution in the low frequency range, in the case of the HZL samples, while LUs represent an important contribution in the 10BBL sample, at low frequency. In all cases, translational self-diffusion dominates the relaxation dispersion in the intermediate frequency regime, as observed in many other SmA systems [dong's book Nuclear Magnetic Resonance spectroscopy...], while fast overall rotations and internal reorientation motions are relevant only in the high frequency range, as shown in **Figure 4(a)**.

The TGBC* phases, which are characterized by in-blocks SmC* phase structure as depicted in **Scheme 1(B)**, are very sensitive to applied magnetic and/or electric fields, and in many cases, the helical SmC* phase structure is unwound within the TGBC* phases. In the HZL mesogens, two types of TGBC* phases were observed [7,9] and, as shown by ^2H NMR investigations [19], both TGBC₁* and TGBC₂* phases have a supramolecular structure not unwound by magnetic fields below 4.2 T, but only partially distorted. The differences between the two TGBC* phases in the mesogen HZL 7/* are rather small, and they are related to the TGB pitch, which is short in the TGBC₁* phase ($\sim 1 \mu\text{m}$) and much longer in the TGBC₂* phase. Because of that, the TGBC₂* phase structure is substantially undistorted and more rigid.

In the analysis of the ^1H NMR relaxation rates in the TGBC₁* phase (see **Figure 4(B)**), we have introduced in-layer fluctuations of the tilting direction (cDF), instead of the layer undulations (LUs) typical of smectic A phases. Moreover, this type of fluctuations is superimposed with the fast reorientational (Rf) so they are treated as a single process. In the intermediate regime, the cDF and SD relaxation mechanisms represent the most important contributions, whereas the RMTD seems to be the most relevant relaxation contribution in the low frequency range. These features can be generalized also in the case of HZL 9/* and partially in the case of 10BBL mesogen. In **Figure 4(C)** the ^1H NMR relaxation dispersions of HZL 7/* in the TGBC₂* phase is also reported. As already stated, this dispersion curve is very different from the others in TGBC*phases (see **Figure 3(B)**). In

particular, in the intermediate frequency regime, the relaxation rate shows a ω^{-1} dependence, which is well fitted by the dominant LU dispersion. Here, the contribution of molecular tumbling could not be estimated since it is partially overlapped with the dominating LU relaxation dispersion. On the other hand, in the fast regime, the self-diffusion is treated together with the fast spinning rotation (SD+Rf), while in the slow frequency regime, the dispersion is well explained by the RTMD model.

Final remarks

In this work, we reviewed the main dynamic features of the TGB phases, as obtained in recent works based on ^1H NMR relaxometry. The analysis of relaxation rates $R_1(T)$ in a wide frequency range (from 100 MHz to 5kHz) in three lactate derivatives (namely HZL 7/*, HZL 9/* and 10BBL) showing TGBA* and TGBC* phases stable in wide temperature intervals allowed us to get interesting information about typical molecular dynamic processes active in these phases. From these studies, we could, in particular, confirm ~~for instance~~ the presence of strong rotations mediated by translational displacements (RMTD) in the slow frequency regime in all TGBA* and TGBC* phases. The high frequency regime is characterized by fast reorientations, which merge with self diffusion (SD) in the case of lower temperature TGBC₂* phase of HZL 7/*. More complicate behavior is observed at intermediate frequency regime. Here, the TGBA* phase is characterized by layer undulations (LUs), which are replaced by in-layer fluctuations of the tilting direction in the SmC* phase (cDF) in the case of TGBC₁* phase of HZL samples, while they are still dominant in the TGBC* phase of 10BBL and in the TGBC₂* phase of HZL 7/* mesogens.

Acknowledgment

This work was partly supported by the “Fast Field-Cycling NMR relaxometry study of chiral and non-chiral nematic liquid crystals” bilateral project Slovenia-Portugal. V.D. thanks the Centre of Excellence NAMASTE (Ljubljana) for the financial support as a visitor professor. The authors V. D., V. N. and V. H. thank the project ASCR M100101204 for partial support.

References

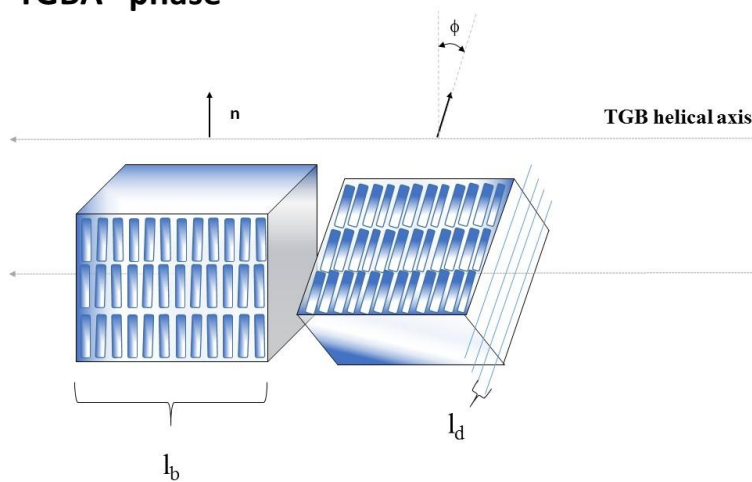
1. Goodby JW: Twist grain boundary and frustrated liquid crystal phases. *Curr. Opin. Coll. Int. Sci.* 2002, **7**, 326-332.
2. Goodby JW, Waugh MA, Stein SM, Chin E, Pindak R, Patel JS: Characterization of a new helical smectic liquid crystal. *Nature.* 1989, **337**, 449-452.
3. Navailles L, Pansu B, Gorre-Talini L, Nguyen HT: Structural study of a commensurate TGB(A) phase and of a presumed chiral line liquid phase. *Phys. Rev. Letts.* 1998, **81**, 4168-4171.
4. Navailles L, Pindak R, Barois P, Nguyen HT: Structural study of the smectic-C twist grain-boundary phase. *Phys. Rev. Letts.* 1995, **74**, 5224-5227.
5. Zhang J, Domenici V, Veracini CA, Dong RY: Deuterium NMR of the TGBA* Phase in Chiral Liquid Crystals. *J. Phys. Chem. B* 2006, **110**, 15193.
6. Domenici V, Veracini CA, Hamplova V, Kaspar M: Supra-Molecular Structure of TGBC* Phases Studied by Means of Deuterium NMR Line-Shape Analysis. *Mol. Cryst. Liq. Cryst.* 2008, **495**, 133.
7. Novotna V, Kaspar M, Domenici V, Hamplova V, Glogarova M, Bilkova P, Pocięca D: Synthesis and mesomorphic properties of new compounds exhibiting TGBA and TGBC liquid crystalline phases. *Liq. Cryst.* 2008, **35**, 287.
8. Kaspar M, Novotna V, Glogarova M, Hamplova V, Pocięca D: New compounds with a TGBA-TGBC-SmC* phase sequence. *Liq. Cryst.* 2010, **37**, 129–137.
9. Apih T, Domenici V, Gradisek A, Hamplova V, Kaspar M, Sebastiao PJ, Vilfan M: ¹H NMR Relaxometry Study of a Rod-Like Chiral Liquid Crystal in Its Isotropic, Cholesteric, TGBA*, and TGBC* Phases. *J. Phys. Chem. B*, 2010, **114**, 11993–12001.
10. Gradisek A, Apih T, Domenici V, Novotna V, Sebastiao PJ. Molecular dynamics in a blue phase liquid crystal: a ¹H fast field-cycling NMR relaxometry study. *Soft Matter*, 2013, **9**, 10746.
11. Figueirinhas LJ, Ferraz A, Ribeiro AC, Noack F, Nguyen HT: Study of the Molecular Dynamics in the TGBA and SC* Mesophases of the Liquid Crystal 18FBTCO1M7. *J. Phys. II*, 1997, **7**, 79–91.

12. Sebastião PJ, Cruz C, Ribeiro AC: Advances in Proton NMR Relaxometry in Thermotropic Liquid Crystals. In *Nuclear Magnetic Resonance of Liquid Crystals*; Dong, R. Y., Ed.; Publisher World Scientific Publishing Co.: Singapore, 2009; Chapter 6.
13. Dong R, Nuclear magnetic resonance of liquid crystals, Springer, New York, 1997.
14. Aluculesei F, Vaca-Chavez C, Cruz C, Sebastiao PJ, Nagaveni NG, Prasad V, Dong RY: Proton NMR relaxation study on the nematic–nematic phase transition in A131 liquid crystal. *J. Phys. Chem. B*, 2012, **116**, 9556–9563.
15. Sebastiao PJ, Gradisek A, Pinto LFV, Apih T, Godinho MH, Vilfan M: Fast field-cycling NMR relaxometry study of chiral and nonchiral nematic liquid crystals. *J. Phys. Chem. B*, 2011, **115**, 14348–14358.
16. Bloembergen N, Purcell EM, Pound RV: Relaxation effects in nuclear magnetic resonance absorption. *Phys. Rev.*, 1948, **73**, 679–712.
17. Vilfan M, Zumer S: Theory of nuclear-spin relaxation by translational self-diffusion in liquid crystals: Smectic A phase. *Phys. Rev. A*, 1980, **21**, 672–680.
18. Torrey HC: Nuclear Spin Relaxation by Translational Diffusion. *Phys. Rev.* 1953, **92**, 962.
19. Domenici V, Veracini CA, Novotna V, Dong RY: Twist grain boundary liquid-crystalline phases under the effect of the magnetic field: A complete H-2 and C-13 NMR study. *Chem Phys. Chem.*, 2008, **9**, 556-566.

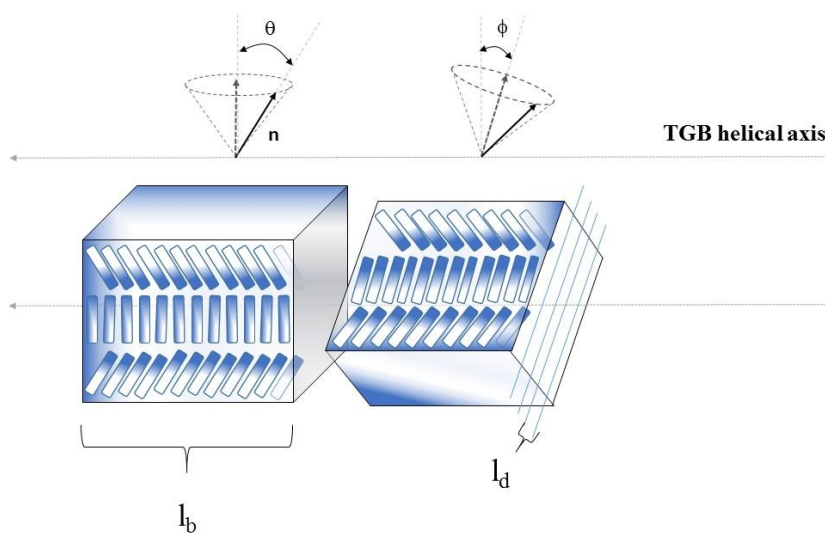
Scheme 1.

Sketch of the TGBA* and TGBC* mesophase structure. The main features of these supramolecular structure are: the presence of TGB helical axis, the dimension of TGB blocks (l_b), the distance between disclinations (l_d), the twist angle (ϕ) between consecutive TGB blocks and the phase director (\mathbf{n}); additionally, in the TGBC* phase, the molecular tilt (θ) with respect to normal to the smectic layer.

TGBA* phase

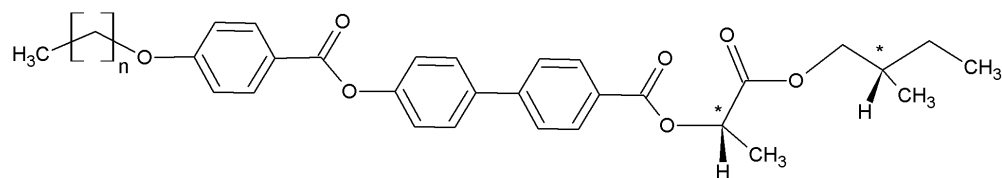


TGBC* phase

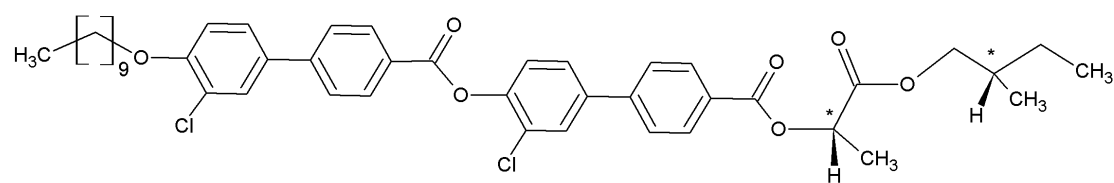


Scheme 2.

Molecular formula of (A) HZL 7/* (n=6) and HZL 9/* (n=8); (B) 10BLL.



(A)



(B)

Figure 1.

Proton NMR spectra of the sample HZL 9/* recorded at 100MHz at different temperatures: (A) 420K, (B) 393K and (C) 340K. The scale is in kHz.

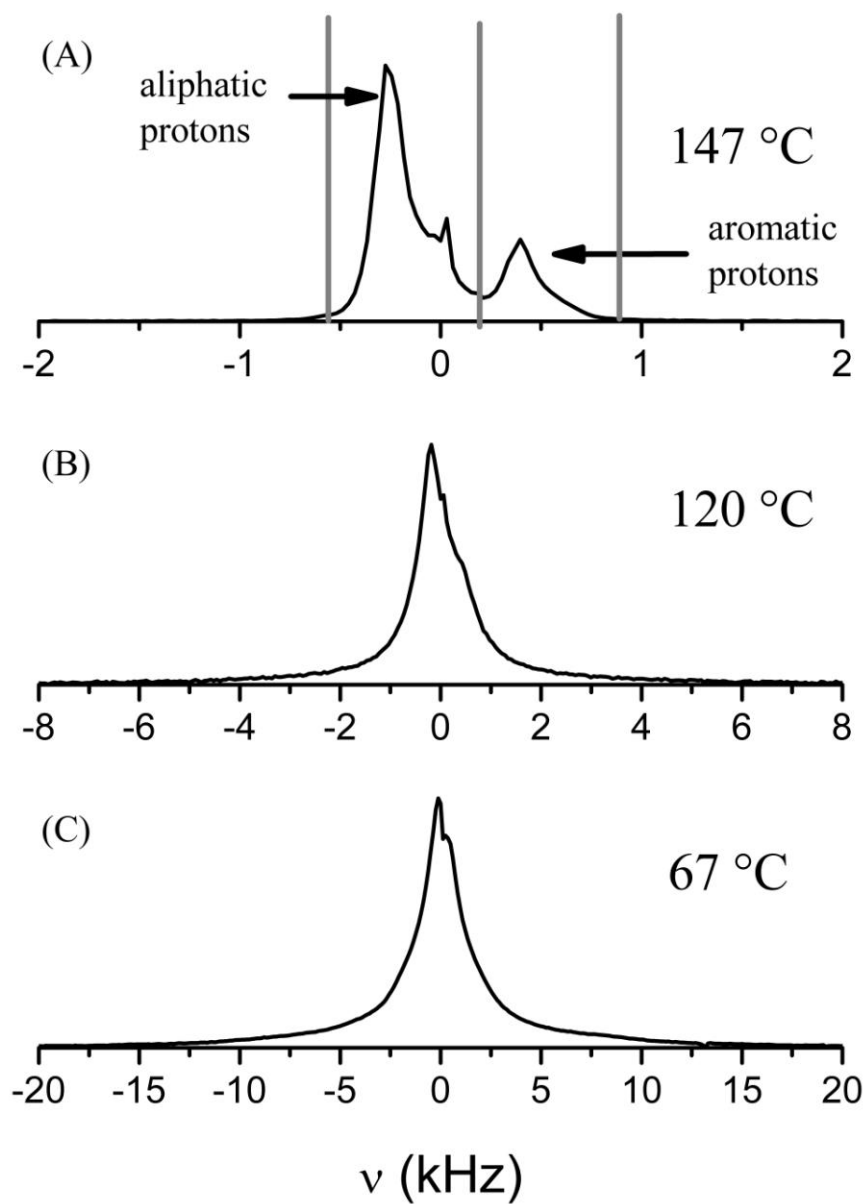
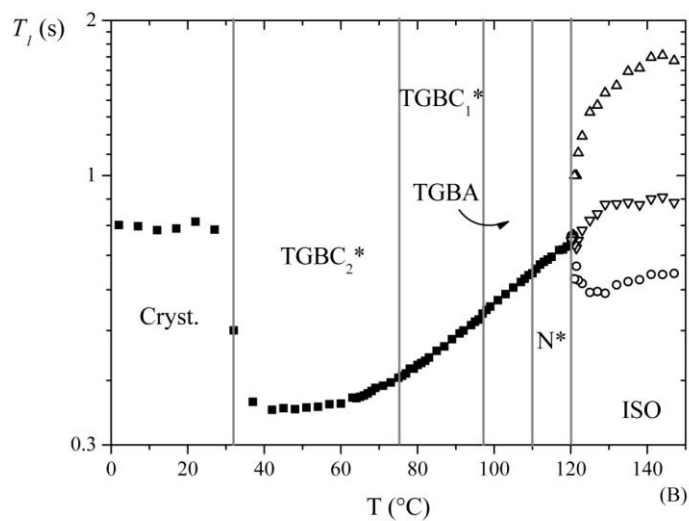
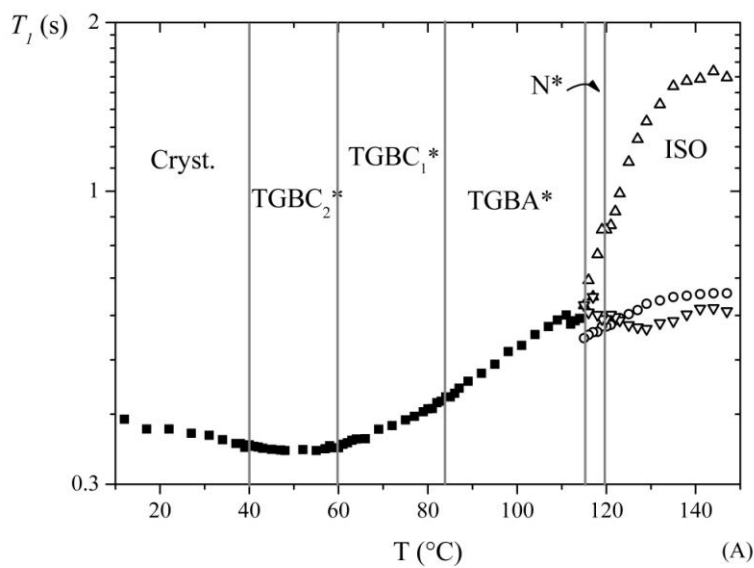


Figure 2.

Temperature dependence of the spin-lattice relaxation time (T_1) at 100MHz of (A) HZL 7/* (B) HZL 9/* and (C) 10BLL mesogens. In the isotropic phase, there are three relaxation components, which are assigned to (\circ) aromatic protons, (\blacktriangle) CH_3 protons and (\blacktriangledown) CH_2 protons. In the liquid crystalline phases and crystal phase there is only one relaxation time (\blacksquare). Temperature transitions and mesophases are indicated as black lines.



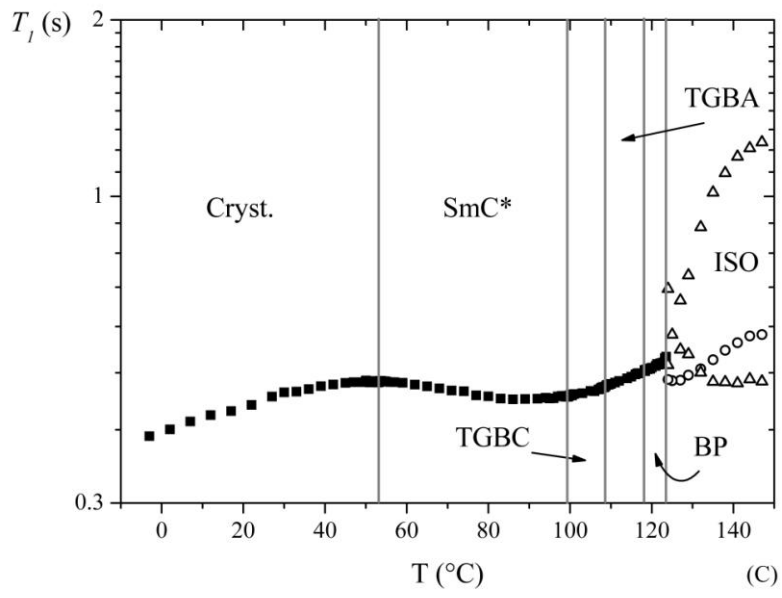


Figure 3.

Selection of dispersion curves (^1H spin-lattice relaxation rates vs Larmor frequency) of the two samples HZL7/* and HZL 9/*. **(A)** In the TGBA* phase: HZL 7/* samples at (■) 111°C and (●) 95°C, HZL 9/* at (□) 106°C and (○) 101°C. **(B)** In the TGBC* phases: HZL 7/* samples at (Δ) 60°C and (□) 40°C, HZL 9/* at (●) 91°C, (■) 84°C and (\blacktriangle) 74°C.

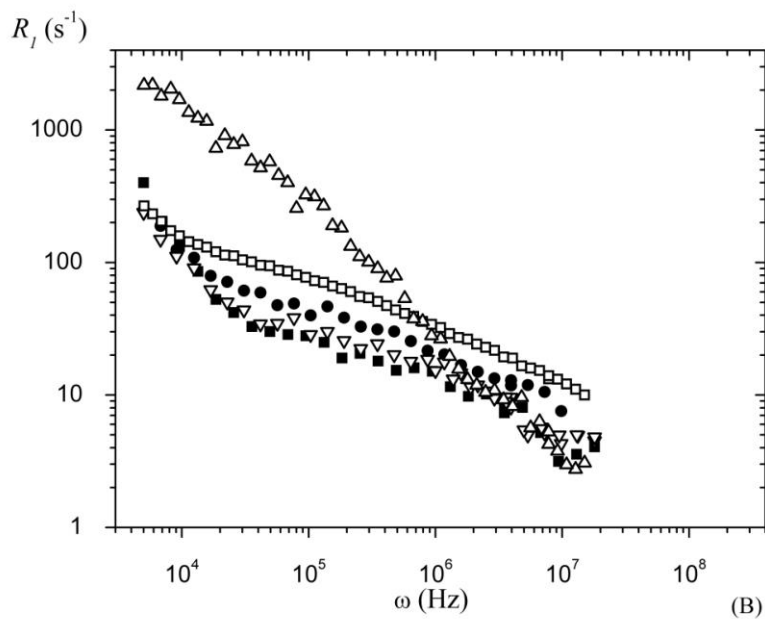
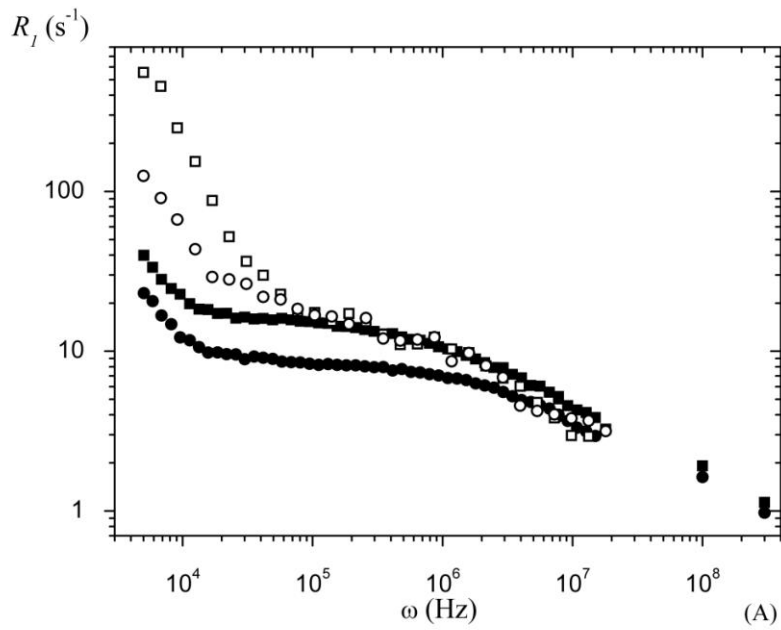


Figure 4.

Frequency dependence of the ^1H spin-lattice relaxation rates in the TGBA* for the sample 10BBL at 113°C (A) and in the TGBC₁* and TGBC₂* for the sample HZL 7/* at 60°C (B) and at 40°C (C), respectively. The empty circles are the experimental data, and the solid black curves are the total fitting curves. Curves for the main dynamic mechanisms are also shown. The free fitting parameters are reported in ref.s [9,10].

